Biosensors and Bioelectronics 58 (2014) 114–120

Contents lists available at ScienceDirect

Biosensors and Bioelectronics

journal homepage: www.elsevier.com/locate/bios

Enhanced antibody recognition with a magneto-optic surface plasmon resonance (MO-SPR) sensor

Maria Grazia Manera [a,*], Elías Ferreiro-Vila [b], José Miguel Garcia-Martin [b], Antonio Garcia-Martin [b], Roberto Rella [a]

[a] CNR-IMM-Institute for Microelectronic and Microsystems, Unit of Lecce, Via per Monteroni, 73100 Lecce, Italy
[b] IMM-Instituto de Microelectrónica de Madrid (CNM-CSIC), Isaac Newton 8, 28760 Tres Cantos, Madrid, Spain

ARTICLE INFO

Article history:
Received 24 November 2013
Received in revised form
29 January 2014
Accepted 3 February 2014
Available online 14 February 2014

Keywords:
Surface Plasmon Resonance (SPR)
Magneto-optic
Transducing layer
Active plasmonics

ABSTRACT

A comparison between sensing performance of traditional SPR (Surface Plasmon Resonance) and magneto-optic SPR (MOSPR) transducing techniques is presented in this work. MOSPR comes from an evolution of traditional SPR platform aiming at modulating Surface Plasmon wave by the application of an external magnetic field in transverse configuration. Previous work demonstrated that, when the Plasmon resonance is excited in these structures, the external magnetic field induces a modification of the coupling of the incident light with the Surface Plasmon Polaritons (SPP). Besides, these structures can lead to an enhancement in the magneto-optical (MO) activity when the SPP is excited. This phenomenon is exploited in this work to demonstrate the possibility to use the enhanced MO signal as proper transducer signal for investigating biomolecular interactions in liquid phase. To this purpose, the transducer surface was functionalized by thiol chemistry and used for recording the binding between Bovine Serum Albumin molecules immobilized onto the surface and its complementary target. Higher sensing performance in terms of sensitivity and lower limit of detection of the MOSPR biosensor with respect to traditional SPR sensors is demonstrated.

1. Introduction

One of the foremost technologies for labeling-free biosensing is based on the Surface Plasmon Resonance (SPR) phenomenon (Liedberg et al., 1995; Schuck, 1997; Garland, 1996). In fact, at a metal–dielectric interface, the free electrons of the metal surface can support a collective oscillation, generating an associated electromagnetic (EM) wave and a Surface Plasmon Polariton (SPP) (Raether, 1988). The field vectors of this EM wave reach their maxima at the interface and decay evanescently into both media. The evanescent field is responsible for the detection of refractive index changes at the metal/dielectric interface. Small variations in the refractive index of the medium located in contact with the metal layer are recorded by changes in the SPR optical signal (Fig.1 a, b).

The SPP oscillations are excited by an external illumination on condition that the wave-vector of the surface plasmon wave matches the photon momentum of light. If a metal film is coated directly on a prism (Kretschmann and Raether, 1968; Cullen et al. 1987–1988; Jorgenson and Yee, 1993; Homola et al., 1999) (Kretschmann geometry), such matching can be achieved by a proper choice of the angle of incidence of a monochromatic light beam onto the prism base.

Biological and chemical analyses are achieved by functionalizing the gold surface with surface bioreceptors and measuring the shift of corresponding optical signals (Homola et al., 1999).As widely reported in the literature, intensity interrogation demonstrates a higher sensitivity with respect to angular interrogation; this is why it is the most common choice for the realization of SPR sensing setup (Zacher and Wischerhoff, 2002; Ran and Lipson, 2006; Kanda et al., 2004; Giebel et al., 1999).

Numerous studies have been carried out to optimize the performance of SPR-based detection technology, owing to the fact that the detection performance of the current practical SPR biosensors is often insufficient to monitor low concentrations of small biomolecular analytes (i.e., drugs, vitamins, and antigens). The optimization of the optical metrology systems or the choice of efficient data analysis methods can lead only to slight improvement in SPR sensing performances. Better results can be obtained by modifying transducers interfaces or modulating the optical signals (Schasfoort and Tudos, 2008; Liedberg et al., 1983; Melendez et al., 1996; Zhang and Uttamchandani, 1988; Karlsson, 2004).

Transducer layers can be modified, for instance, by adding a nanostructuration on the metal sensing layer: localized SPR (LSPR) using periodic nanowires and nanoposts as well as sub wave-

* Corresponding author. Tel.: +39 832 422523.
E-mail address: mariagrazia.manera@le.imm.cnr.it (M.G. Manera).

http://dx.doi.org/10.1016/j.bios.2014.02.003
0956-5663

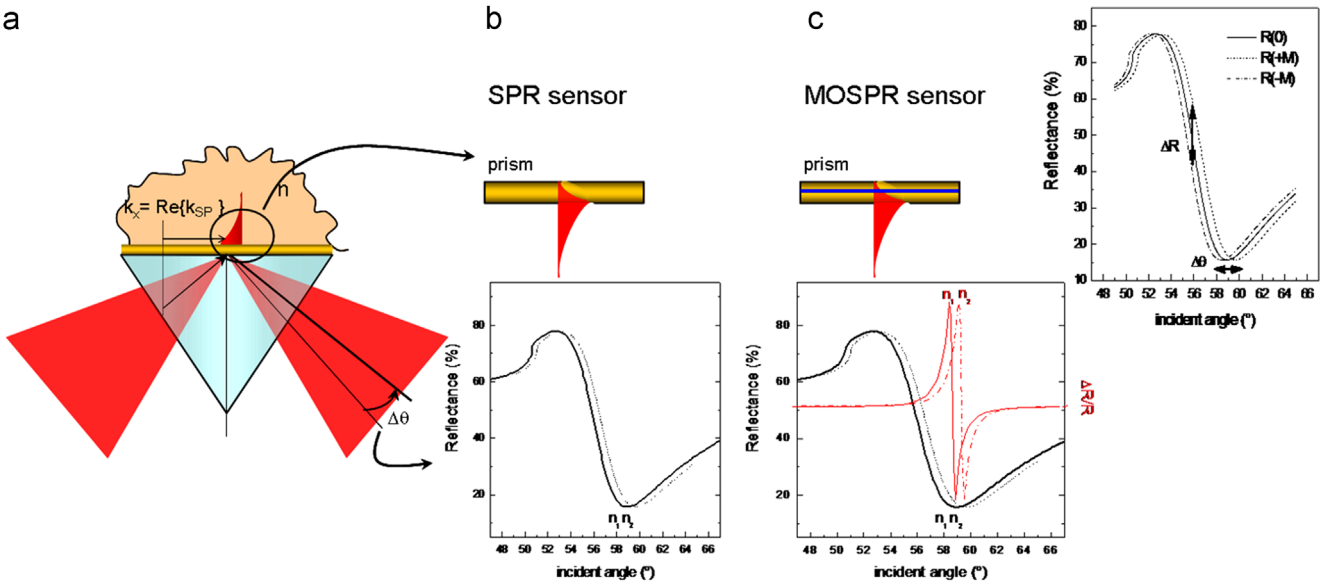

Fig. 1. (a) Schematic representation of the experimental setup for SPR excitation in Kretschmann configuration; (b) detail of the metal transducer/dielectric interface of a standard SPR sensor and excitation of surface plasma wave exponentially decaying into the dielectric. The changes in SPR curves upon a change in refractive indexes $n_1 < n_2$ is also shown; and (c) detail of the hybrid metal/ferromagnetic/metal trilayer transducer of a MOSPR sensor and excitation of surface plasmon wave exponentially decaying into the dielectric. The EM field is enhanced at the MO active layer, thus enhancing the magneto-optical signal. A schematic response of SPR and MOSPR signal to the same change in refractive index is reported. The graph on the right shows the effect of the reverse of magnetization on the SPR curve, namely on the angular minima shift $\Delta\theta$ and on the reflectance ΔR.

length nanogratings deposited onto metal surfaces can be used (Moon et al., 2010; Kim et al., 2006; Byun et al., 2007; Malic et al., 2007). Further examples can include signal amplification using functionalized nanoparticles (He et al., 2000), or using the combination of metal nanoparticles and dielectric materials. In the latter cases sensing improvements are due to the possibility to enhance SPs capabilities and increase its ability to sense small analyte molecules. Such modifications of transducer interfaces are responsible for the enhancement of the electromagnetic field (EM) in the close vicinity of the metal transducer layer (Nenninger et al., 2001); hence, increasing the sensitivity of the biosensor when compared to traditional interfaces.

On the other hand, external modulation techniques can be used to improve the signal-to-noise (SNR) ratio of the SPR sensing measurements, thus increasing the limit of detection (LOD) with respect to traditional SPR sensors. For this purpose, the mechanical (Hooper and Sambles, 2004; Patskovsky et al., 2008) and the phase (Wu et al., 2003; Markowicz et al., 2007; Kabashin et al., 2009) modulated SPR sensors have been proposed in the literature.

In this work, the idea is to use both modification of traditional SPR transducer layer and modulation of SPR signal in order to get significant increase in sensitivity with respect to standard SPR sensors. For this purpose Au/Co/Au trilayers were used as transducer, and the magnetic modulation of the plasmon wave vector was used as the sensor signal (Fig. 1c). The modulated nature of the signal together with a proper choice of metal and ferromagnetic trilayer tailored on the nanoscale will ensure the achievement of the goal of the work.

Different papers have reported the possibility of controlling SPP excitations in metallic trilayer structures by means of an external magnetic field (González-Díaz et al., 2007; Ferreiro-Vila et al., 2009; Armelles et al., 2009). When the SPP is excited in these structures, an external magnetic field can induce a modulation in the SPP wavevector, provided that the magnetic field is applied perpendicularly to the direction of propagation of the SPP and parallel to the interface. In addition, an enhancement in the magneto-optical (MO) activity is evidenced when the SPP is excited in these structures (González-Díaz et al., 2007; Armelles et al., 2009; Armelles et al., 2013; Wallis et al., 1974; Hermann et al., 2001; Armelles et al., 2008).

The amplified MO signal induced by the excitation of the SPP is chosen as sensor signal which is able to record biomolecular interactions occurring at the metal/dielectric interface. For this purpose, a simple experimental setup is required, based on intensity interrogation provided with magnetic actuation in a transverse configuration. A small electromagnet producing a proper magnetic field intensity can be used for this purpose. These multilayered structures, showing both plasmonic and magneto-plasmonic activity, have been demonstrated to be used as proper new transducers in a MOSPR gas sensor (Manera et al., 2011; Sepúlveda et al., 2006; Regatos et al., 2010; Regatos et al., 2011; Manera et al., 2012).

In this work, by investigating a simple bioassay experiment, we demonstrate that this new strategy can be used to enhance SPR biosensor sensitivity. Biosensing measurements obtained in this work give us a complete view of functional characterizations carried out by using these novel transducers; the work extends in liquid phase our previous sensing results performed on gaseous environment.

2. Materials and methods

2.1. Materials

N-hydroxysuccinimide(NHS), N-(3-dimethylamino- propyl)-N0-ethylcarbodiimide hydrochloride (EDAC), ethanolammine and11-mercaptoundecanoicacid (11-MUA), Bovine serum albumin (BSA) and the corresponding antibody anti-BSA (a-BSA) were purchased from Sigma-Aldrich. Hybridization measurements were performed using a saline phosphate-buffer (PBS, pH 7.4). Deionized water was used for the preparation of all solutions.

2.2. Preparation of plasmonic and magneto-optical transducing layers

Transducer layers were composed of 15 nm Au (capping) /6 nm Co/25 nm Au/2 nm Ti deposited on SF10 glass substrates. They were deposited by dc magnetron sputtering at room temperature in an

ultrahigh-vacuum chamber with a base pressure of 10^{-9} mbar. In these conditions all the layers are polycrystalline and the Co layer has in-plane magnetization. The 2 nm thick Ti layer between the substrate and the 25 nm Au layer has a role to improve the adherence of the magnetoplasmonic structure to the glass substrate.

The thickness values were chosen in order to maximize the magneto-optical ΔR signal upon the change in the real part of refractive index n (González-Díaz et al., 2007) while preventing Co oxidation.

For the sake of comparison, a set of 50 nmAu/2 nm Ti layers were also deposited onto SF10 glass substrate by consecutive thermal evaporation. This set of transducers was used for traditional SPR experiments carried out in parallel with respect to MOSPR measurements.

2.3. SPR and MOSPR characterization techniques

Surface Plasmon Polaritons (SPPs) are charge density oscillations, which may propagate along the interface between two media with dielectric constants of opposite sign (e.g., metal–dielectric interface). Surface Plasmon Resonance (SPR) is the optical excitation of these charge-density oscillations.

Generally, a two-phase system consisting of a metal and a dielectric, can be analyzed by using Maxwell's equations, yielding the dispersion relation:

$$k_{spp} = k_0 \sqrt{\frac{\varepsilon_m \varepsilon_d}{\varepsilon_m + \varepsilon_d}} \quad (1)$$

where k_{spp} is the wave-vector of a Plasmon, ε_m is the dielectric constant of the metal at frequency ω and ε_d is the dielectric constant of the dielectric medium (sample), k_0 is the wavevector of light in vacuum (Homola et al., 1999).

Now, if a magnetic field is applied perpendicular to the direction of propagation of the SPP and parallel to the interface, it will necessarily modify the SPP wavevector. In simple structures such as dielectric/ferromagnetic and dielectric/ferromagnetic/dielectric layers, the SPP wavevector modification will depend linearly on both the film thickness and the values of the nondiagonal elements of the dielectric tensor (Kushwaha and Halevi, 1987).

As a consequence of the SPP wave-vector change, the angle at which the SPP excitation is obtained changes as well. When the magnetization of the ferromagnetic layer is reversed from a value $+M$ to $-M$, the variation of the SPR angle can be expressed by

$$\Delta\theta = [\theta(+M) - \theta(-M)]. \quad (2)$$

The angular shift obtained is proportional to the wavevector variation of the SPP excitation condition induced by the magnetization inversion Δk_{SPP}

$$\Delta\theta = \frac{\Delta k_x}{n k_0 \cos\theta} \quad (3)$$

This variation translates into a modification of the reflectance signal ΔR than can be approximated by the following Eq.

$$\Delta R = R(+M) - R(-M) = \frac{\partial R}{\partial \theta} \times \Delta\theta \quad (4)$$

where $\Delta\theta$ is the same as defined by Eq. (2).

The latter is translated into a relative variation in the reflected p-polarized light (R), which is related to the Transverse Magneto-optic Kerr effect (TMOKE)

$$\frac{\Delta R}{R} = \frac{R(M) - R(-M)}{R(0)} \quad (5)$$

More detailed information about the theoretical aspects can be found in references (González-Díaz et al., 2007; Ferreiro-Vila et al., 2009).

Taking into account that SPP wavevector depends on the optical properties of the metal/dielectric interface, both R and modulated ΔR signals can be used as a novel transducer probes for the monitoring of optical changes at the metal/dielectric interface (Fig. 1). The modulated nature of the MO signals is expected to ensure a high signal-to-noise ratio which will put into higher sensitivity values.

2.4. SPR and MOSPR experimental setups

A home-made experimental set-up using Kretschmann's prism configuration was used for traditional SPR measurements (Fig. 1). An index-matching fluid was used to bring an optical contact between the glass substrate and the prism (refractive index $n=1.7$, determined by Brewster angle measurement). Surface plasmon excitation was achieved by focusing a p-polarized He–Ne monochromatic laser source ($\lambda=632.8$ nm) onto the prism/sample interface. The incidence angle of light beam is chosen by rotating the prism/sample combination, placed on a θ–2θ rotation table driven by a microprocessor-controlled stepping motor (with a resolution of 0.01°). The reflected light is detected by a Si photodiode.

An electromagnet was placed perpendicular to the prism/sample combination. It produces an alternating magnetic field (intensity: 30 Oe and frequency: 800 Hz) that lies in the plane of the Co layer and is perpendicular to the plane of incidence of light. The modulated signal was processed by a pre-amplifier and then by a lock-in amplifier which allowed extracting the variation of the reflected intensity signal at the specific reference frequency removing the noise due to other frequencies.

A peristaltic pump was used to deliver the investigated solution into an home-made test chamber (volume: 10 μl). All experiments were carried out at room temperature.

2.5. Calibration to refractive index changes

In order to enable comparison of different experiments, the sensor response was calibrated to bulk refractive index changes. Four refractive indexes standard solutions were prepared by ethanol diluted in deionized water. The refractive indexes were from 1.33289 to 1.33639, corresponding to volume concentrations of 5, 10, 20, 30, 40, 50 % (v/v).

2.6. Sensor chip functionalization and biosensing assay

Before the immobilization of the probe, the metal transducers were washed in a boiling solution of H_2O_2 (30%), NH_3 (30%) and milliQ water in a 1:1:5 ratio for 10 min and then rinsed with milliQ water.

Plasmonic and magneto-plasmonic multilayer transducers were submerged into a glycerol/ethanol (1:1, v/v) solution containing 150 mM 11-mercaptoundecanoic acid (11-MUA) overnight (Yam et al., 2001). The carboxylic group of 11-MUA was activated by a solution of 50 mM NHS for 10 min followed by 30 mM EDAC at the same concentration, in recycle for 30 min in water/ethanol (10/1, v/v). A self-assembled monolayer of BSA was obtained by incubation of the activated transducer substrate in a solution of 50 ppm in ultra pure water. Remaining active sites were blocked using ethanolamine (1 M). Hence, different solutions of anti-BSA antibodies at different concentrations were allowed to flow over the sensor surface (interaction time 15 min).

For the regeneration of the sensor surface, HCl solution was used (10 mM).

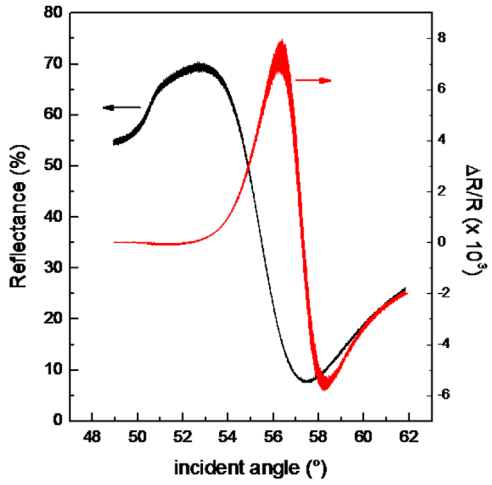

Fig. 2. Experimental reflectivity curve (R vs. angle) and Magneto-optic curve ($\Delta R/R$ vs. angle) of Au/Co/Au multilayers deposited on SF10 glass substrates. The experimental curves are recorded when deionized water is present into the test chamber.

3. Results and discussions

3.1. SPR and MOSPR characterization

All samples exhibited low saturation field (around 30 Oe), as expected for a Co thin layer of a few nanometer thick. Transverse Magneto-optic Kerr effect (TMOKE) loops have been reported in Ref. (González-Díaz et al., 2007).

In Fig. 2 the angular dependence of the reflectivity of the investigated Au/Co/Au transducer together with the relative variation of the reflectivity ($\Delta R/R$) induced by the magnetic field actuation, are recorded in water medium. As shown, the angular variation of the reflectivity shows firstly total internal reflection at 50.7° and then the SPP excitation with the clearly observed minimum at 57.5°. Also the magneto-optic $\Delta R/R$ signal is characterized by a sharp resonance in the angular behavior around such as a value, i.e. when the SPP is excited. In absence of resonance condition, both R and $\Delta R/R$ are basically constant in the same angular range (see for instance (González-Díaz et al., 2007)).

For angular positions where the SPP is excited, the EM field gradually increases from the glass incident light side reaching as expected a maximum value at the air–Au interface, where the SPP is located (Homola et al., 1999) (Fig. 1). This implies that the EM field is drastically enhanced at the MO active layer region, being responsible for the enhancement of the magneto-optical signal. Maximal changes in the magneto-optical signal will occur in the angular region of the minimum of the SPR curve where the probing electric field is maximal, whereas maximal reflectivity changes are observed on the resonance slopes.

Like SPR curve, also magneto-optical curve will be able to sense refractive index changes at metal–dielectric interface (Fig. 1). As the MO signal can experience a much steeper change across the plasmon resonance region than reflectivity curve (Fig.2), we expect that it is more sensitive to small variations of refractive index than reflectivity measurements.

3.2. Refractometry

A refractometric experiment was performed by sending into the test chamber liquid samples with different refractive indexes and recording the corresponding change in the sensor signal.

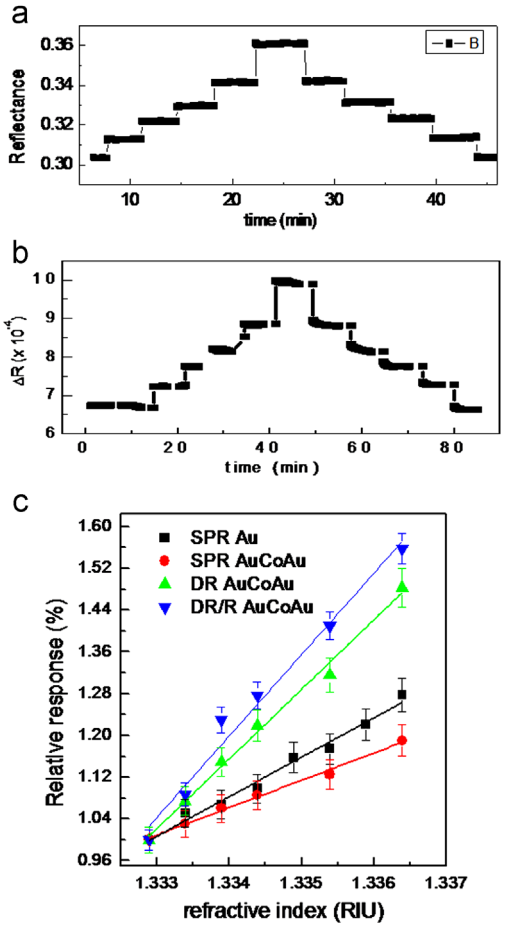

Fig. 3. Experimental refractometric measurement carried out sending into the test chamber different concentrations of ethanol solutions for a SPR (a)MOSPR (b) sensor and calibration curves (c).

For this purpose, a set of ethanol solutions prepared in deionized water with different refractive indexes were used.

Fig. 3(a) and (b) shows the changes in both SPR and MOSPR sensor signals when different concentrations of the ethanol solutions were poured into the test chamber. In Fig. 3c the corresponding calibration curves are reported. Here the sensor response is intended as the ratio of the intensity of the investigated sensor signals in presence of the analyte and the signals recorded in water.

From the slopes of the calibration curves, the bulk refractive index sensitivity was determined to be approximately 52 RIU^{-1}, 133 RIU^{-1}, 155 RIU^{-1} (RIU: Refractive Index Unit) within the whole range of measured refractive indexes, for the sensor using R, ΔR and $\Delta R/R$ as sensor signals, respectively.

For a complete comparison, also refractometric measurements were carried out with a bare Au transducer, which is the optimum transducer for a standard SPR experiment, reflectance R being the sensor signal in this case . The calculated sensitivity is 75 RIU^{-1}.

A two-fold improvement in sensing performance can be seen when using magneto-plasmonic transducers with both ΔR and $\Delta R/R$ signals as sensor signals compared to SPR sensing with Au layer transducer alone.

3.3. Biosensing assay

Once the MOSPR system is calibrated, a comparison between traditional SPR and MOSPR techniques was performed for the monitoring of specific binding reaction between bovine serum albumin (BSA) antigen and the correspondent antibody. The

transducers used in this study were MOSPR transducer Au/Co/Au/Ti/glass, and traditional SPR transducer Au/Ti/glass.

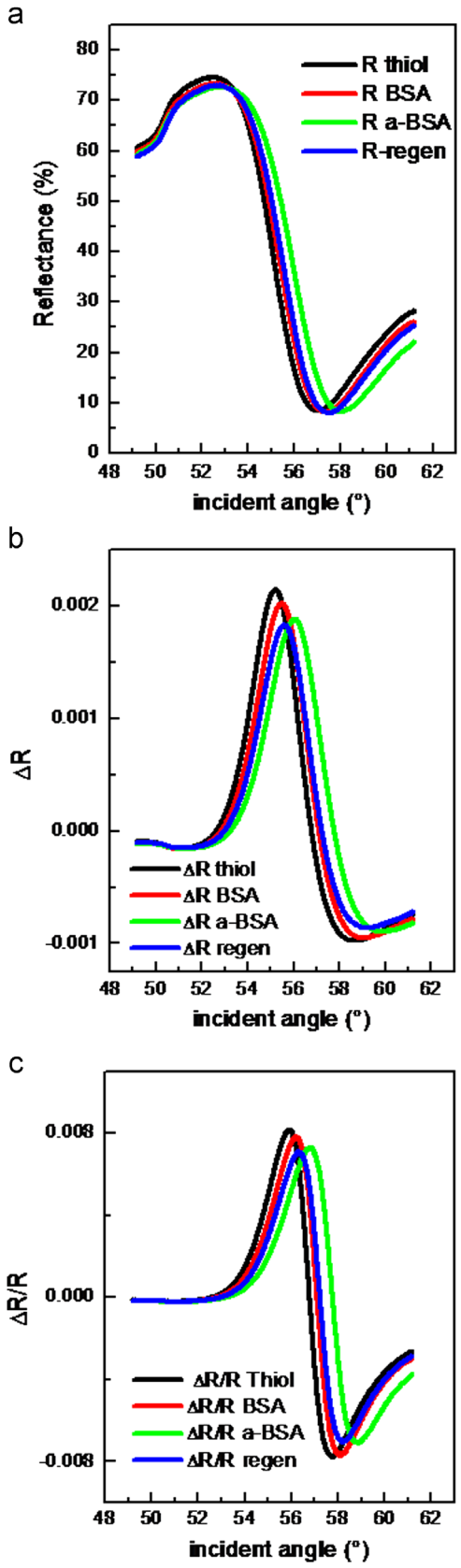

Fig. 4. SPR (a) and MOSPR (b and c) curves recorded for each step of the biosensing assay, namely after thiol functionalization, BSA immobilization, anti-BSA binding and finally regeneration of the sensor.

Fig. 4 reports the SPR reflectivity curves and MOSPR ΔR and relative $\Delta R/R$ curves recorded for each step in the biosensing assay, namely after thiol functionalization, BSA immobilization, anti-BSA hybridization and regeneration steps, respectively. As can be noticed, surface modification of the transducers resulted in an angular shift of the recorded curves towards higher angles. Thiol functionalization, as well as BSA immobilization and consequent hybridization with the corresponding antibody give rise to a change, namely an increase of refractive index at the interface of Au/water which is responsible for the change in the angular positions of SPR and MOSPR curves. Both SPR and MOSPR angular curves were also able to record biosensor surface regeneration. This latter step allowed releasing the binding between BSA and the corresponding antibodies, thus restoring the surface with BSA molecules still present onto the surface. A series of 4 cycles of HCl solution was performed in order to allow a complete regeneration of the sample.

In Fig. 5 the dynamic evolution of the ΔR MOSPR signals upon immobilization of BSA molecules and consequent hybridization of the anchored probes with the target antibodies are shown. The working angle chosen for dynamic measurements was 56° corresponding to the highest slope of the angular curve.

In Fig. 5a the different steps involved in the immobilization of BSA molecules are described in more details. The immobilization phase started with preliminary cycles of a solution with 10% ethanol in water and pure water to clean the sample surface and to get a stable baseline of the signal for MOSPR sensing. Then, the mixture of NHS/EDC (introduced to activate the thiol surface) gave rise to the highest variation of the refractive index in the test chamber. After that, the sample was cleaned with a solution of 10% ethanol in water and pure water. Finally, an aqueous solution of 50 ppm of BSA protein was sent into the test chamber and left

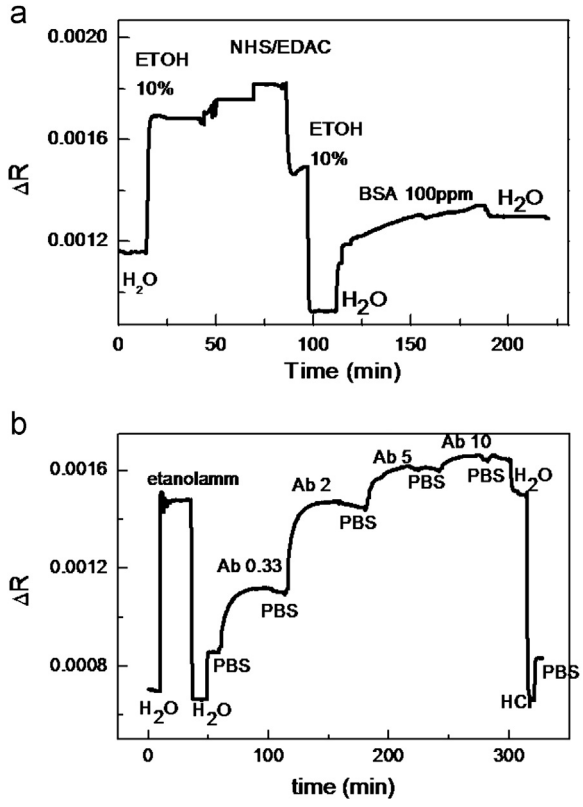

Fig. 5. Dynamic ΔR curves in the MO-SPR sensor recording (a) the activation of the surface by NHS/EDAC solution and BSA immobilization after a proper washing in air, and (b) the binding with increasing concentration of anti-BSA antibodies (Ab) and regeneration step.

in dynamic condition for 20 min, prior washing in pure water. After washing, the sensor signals remained almost unchanged, thus ensuring that BSA cannot be removed and therefore it was correctly immobilized onto the transducer surface ; Fig. 5b describes the hybridization phase. After a washing step in water, ethanolamine (1 M) was introduced in order to block the surface of non-specific interactions from the target biomolecule. After switching back to the PBS buffer solution, the anti-BSA solution was injected into the sensor flow-cell: a fast increase in the MO signals occurred. This increase is associated with the specific binding between BSA and anti-BSA molecules at the sensor surface. The difference between this new level and initial baseline is associated with the amount of bound anti-BSA. For higher anti-BSA concentrations, the initial fast binding was followed by a slower binding, thus demonstrating a kind of saturation in the sensor surface towards further anti-BSA binding. The analog sequence of experimental step recorded by the normalized MOSPR signal ΔR/R is reported in Fig. S1 of Supporting information.

Fig. 6 reports the corresponding calibration curves for all tested sensors. In order to compare all the recorded signals and take into account the different nature and consequent operation range of the sensors signal, the sensor response has been defined as the ratio of the signal intensity at the steady state corresponding to each analyte concentration (0.3, 2, 5, 10 ppm) and the baseline signal recorded in the buffer solution before the first analyte injection.

It can be noticed, the normalized MOSPR signal $\Delta R/R$ gives the highest sensor response for all the investigated analyte concentration ranges. By narrowing the focus on the linear part of the calibration curve, the normalized $\Delta R/R$ signal also reports the highest slope, namely the highest sensitivity. This means that it is more able to record small variations in the antibodies concentration.

On the other hand, non-normalized ΔR signal gives the best signal-to noise ratio value, equal to 279 much higher with respect to the normalized signal (44) and to the bare SPR signal (0.9). A lower limit of detection can be also extracted for MOSPR signals, equal to 6×10^{-2} ppm and 3×10^{-2} ppm for the $\Delta R/R$ and ΔR signals, respectively. On the contrary, standard SPR signal is able to reach only 0.2 ppm. The limit of detection was estimated based on the sensor signal corresponding to three times the standard deviation of the baseline (LOD$=3\sigma/S$, where S is the sensitivity and σ is the standard deviation of the baseline signal) (Hastings, 2008).

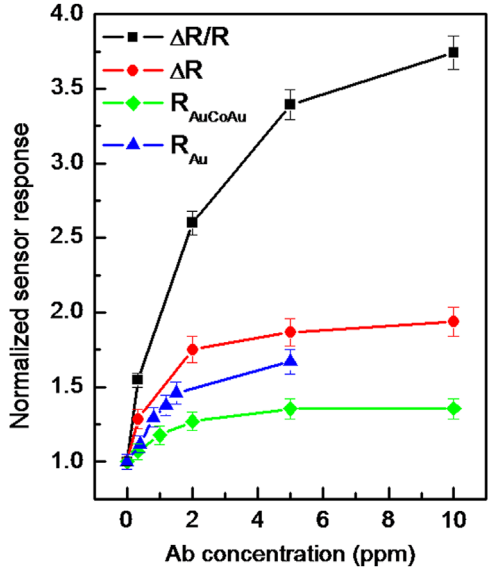

Fig. 6. Calibration curves relative to antibodies (Ab) detection recorded by ΔR/R (squares), ΔR (circles) and reflectivity (rhombs) signals by using as optical and magneto-optical transducer the Au/Co/Au/Ti trilayer. A comparison with reflectivity sensor signal obtained also with a "classical" Au/Ti optical transducer (triangles) is reported.

For the sake of completeness, Fig. 6 also reports the calibration curve relative to a "standard" SPR sensor, namely a SPR sensor using as transducer layer a Ti/Au bilayer deposited onto SF10 glass substrate, as found in most of SPR configurations. The same biosensing assay experimented onto this "standard" transducer allowed recording higher sensitivity with respect to the SPR configuration using a Au/Co/Au multilayer transducer for all investigated concentrations range, but in any case smaller if MOSPR sensing probe is monitored. Lower performance can be also found in the determination of the limit of detection equal to 0.15 ppm, in line to previous results relative to SPR sensors using the Au/Co/Au trilayer as transducer. Each measurements were repeated three times obtaining a good reproducibility (better than 90% for all tested sensors).

4. Conclusions

A set of trilayers composed of a proper choice of metal and ferromagnetic materials was tested as sensor transducers in a MOSPR sensor. The proposed new MOSPR sensing probe is strictly linked to the amplified MO signal induced by the excitation of the SPP at the metal/dielectric interface.

A comparison between the sensing performance of the prepared multilayers in standard SPR and MOSPR sensing experiments has been presented, as well as compared to the performance of a "classical" Au film deposited on glass in a standard SPR configuration. To this purpose, a refractometric study and a simple biosensing assay have been proposed. Both the chemical immobilization of Bovine serum albumin proteins onto the transducer surface and of the binding with the respective antibodies at increasing concentrations by the two sensor signals were monitored.

Increase in biosensing sensitivity of the MOSPR sensor over traditional SPR configuration is put as evidence. In particular ΔR signal results the best choice in terms of accordance between sensitivity and noise value, allowing calculating a limit of detection equal to 0.06 ppm, an order of magnitude better with respect normalized MOSPR and SPR signals.

Acknowledgments

The authors want to acknowledge prof. Alfonso Cebollada and prof. Gaspar Armelles (IMM-CSIC) for the preparation of magneto-plasmonic transducers and for their scientific support, Dr. Enrico De Lorenzis (Biotecgen s.r.l.) and Flavio Casino (IMM-CNR) for their technical support during the biosensing measurements. The authors acknowledge the financial support from the Spanish MINECO under projects MAT2011-29194-C02-01 and CSD2008-00023, the EC through FP7-214107-2 NANOMAGMA, the Italian MIUR through FIRB project RBFR10OAI0 Nanoplasmag and Euro trans-BIO project A12/1992/02/X15 - SPRAI.

Appendix A. Supporting information

Supplementary data associated with this article can be found in the online version at http://dx.doi.org/10.1016/j.bios.2014.02.003.

References

Armelles, G., Cebollada, A., Garcia-Martin, A., Garcia-Martin, J.M., Gonzalez, M.U., Gonzalez-Diaz, J.B., Ferreiro-Vila, E., Torrado, J.F., 2009. J.Opt. A: Pure Appl. Opt. 11, 114023.

Armelles, G., Cebollada, A., Garcia-Martin, A., Gonzalez, M.U., 2013. Adv. Opt. Mat. 1, 10–35.

Armelles, G., González-Díaz, J.B., García-Martín, A., García-Martín, J.M., Cebollada, A., González, M.U., Acimovic, S., Cesario, J., Quidant, R., Badenes, G., 2008. Opt. Express 16, 16104–16112.

Byun, K.M., Yoon, S.J., Kim, D., Kim, S.J., 2007. Opt. Lett. 32, 1902–1904.

Cullen, D.C., Brown, R.G.W., Lowe, C.R., 1987–1988. Biosensors 3, 211–225.

Ferreiro-Vila, E., González-Díaz, Juan, B., Fermento, R., González, M.U., García-Martín, A., García-Martín, J.M., Cebollada, A., Armelles, G., 2009. Phys. Rev. B 80 (12), 125132.

Garland, P.B., 1996. Q. Rev. Biophys. 29, 91–117.

Giebel, K.F., Bechinger, C., Herminghaus, S., Riedel, M., Leiderer, P., Weiland, U., Bastmeyer, M., 1999. Biophys. J. 76 (1), 509–516.

González-Díaz, J.B., García-Martín, A., Armelles, G., García-Martín, J.M., Clavero, C., Cebollada, A., Lukaszew, R.A., Skuza, J.R., Kumah, D.P., Clarke, R., 2007. Phys. Rev. B 76, 153402.

Homola, J., Yee, S.S., Gauglitz, G., 1999. Sens. Actuators B 54, 3–15.

He, L., Musick, M.D., Nicewarner, S.R., Salinas, F.G., Benkovic, S.J., Natan, M.J., Keating, C.D., 2000. J. Am. Chem. Soc. 122, 90719077.

Hooper, I.R., Sambles, J.R., 2004. Appl. Phys. Lett. 85, 3017–3019.

Hermann, C., Kosobukin, V.A., Lampel, G., Peretti, J., Safarov, V.I., Bertrand, P., 2001. Phys. Rev. B 64, 235422.

Hastings, J.T., 2008. IEEE Sens. J. 8, 170–175.

Jorgenson, R.C., Yee, S.S., 1993. Sens. Actuators B 12, 213–220.

Kretschmann, E., Raether, H., 1968. Zeitschrift Fur Naturforschung Part A-Astrophysik Physik Und Physikalische Chemie A 23, 2135–2136.

Kanda, V., Kariuki, J.K., Harrison, D.J., McDermott, M.T., 2004. Anal. Chem. 76 (24), 7257–7262.

Karlsson, R., 2004. J. Mol. Recognit. 17 (3), 151–161.

Kim, K., Yoon, S.J., Kim, D., 2006. Opt. Express 14, 12419–12431.

Kabashin, A.V., Patskovsky, S., Grigorenko, A.N., 2009. Opt. Express 17, 21191–21204.

Kushwaha, M.S., Halevi, P., 1987. Phys. Rev. B 36, 5960.

Liedberg, B., Nylander, C., Lundstrom, I., 1995. Biosens. Bioelectron. 10, i–ix.

Liedberg, B., Nylander, C., Lundstrum, I., 1983. Sens. Actuators B Chem. 4 (1), 299–304.

Melendez, J.L., Carr, R., Bartholomew, D.U., Kukanskis, K.A., Elkind, J., Yee, S.S., Furlong, C.E., Woodbury, R.G., 1996. Sens. Actuators B Chem. 35 (1-3), 212–216.

Moon, S., Kim, D.J., Kim, K., Kim, D., Lee, H., Lee, K., Haam, S., 2010. Appl. Opt. 49, 484–491.

Malic, L., Cui, B., Veres, T., Tabrizian, M., 2007. Opt. Lett. 32, 3092–3094.

Markowicz, P.P., Law, W.C., Baev, A., Prasad, P.N., Patskovsky, S., Kabashin, A., 2007. Opt. Express 15, 1745–1754.

Manera, M.G., Montagna, G., Ferreiro-Vila, E., González-García, L., Sánchez-Valencia, J.R., González-Elipe, A.R., Cebollada, A., Garcia-Martin, J.M., Garcia-Martin, A., Armelles, G., et al., 2011. J. Mater. Chem. 21, 16049–16056.

Manera, M.G., Ferreiro-Vila, E., Cebollada, A., García-Martín, J.M., García-Martín, A., Giancane, G., Valli, L., Rella, R., 2012. J. Phys. Chem. C 116, 10734–10742.

Nenninger, G.G., Homola, J., Yee, S.S., Tobiska, P., 2001. Sens. Actuators B 74, 145–151.

Patskovsky, S., Maisonneuve, M., Meunier, M., Kabashin, A.V., 2008. Opt. Express 16, 21305–21314.

Raether, H., 1988. Surface Plasmons on Smooth and Rough Surfaces and on Gratings. Springer-Verlag, Berlin

Ran, B., Lipson, S.G., 2006. Opt. Express 14 (12), 5641–5650.

Regatos, D., Fariña, D., Calle, A., Cebollada, A., Sepúlveda, B., Armelles, G., Lechuga, L. M., 2010. J. Appl. Phys. 108 (5), 054502.

Regatos, D., Sepúlveda, B., Fariña, D., Carrascosa, L.G., Lechuga, L.M., 2011. Opt. Express 19 (9), 8336–8346.

Schuck, P., 1997. Annu. Rev. Biophys. Biomol. Struct. 26, 541–566.

Schasfoort, R.B.M., Tudos, A.J. (Eds.), 2008. Handbook of Surface Plasmon ResonanceRoyal Society of Chemistry, London, pp. 284

Sepúlveda, B., Calle, A., Lechuga, L.M., Armelles, G., 2006. Opt. Lett. 31, 1085–1087.

Wu, C.-M., Jian, Z.-C., Joe, S.-F., Chang, L.-B., 2003. Sens. Actuators B 92, 133–136.

Wallis, R.F., Brion, J.J., Burstein, E., Hartstein, A., 1974. Phys. Rev. B 9, 3424.

Yam, C.M., Zheng, L., Salmain, M., Pradier, C.M., Marcus, P., Jaouen, G., 2001. Colloids Surf. B 21, 317–327.

Zacher, T., Wischerhoff, E., 2002. Langmuir 18 (5), 1748–1759.

Zhang, L.M., Uttamchandani, D., 1988. Electron. Lett. 24, 1469–1470.